EUKARYOTIC CELL, Oct. 2004, p. 1217–1226 Vol. 3, No. 5
1535-9778/04/$08.00+0 DOI: 10.1128/EC.3.5.1217–1226.2004

A β-Tubulin Mutation Selectively Uncouples Nuclear Division and Cytokinesis in *Tetrahymena thermophila*

Joshua J. Smith,[1]†‡ J. Sebastian Yakisich,[2]† Geoffrey M. Kapler,[2] Eric S. Cole,[3] and Daniel P. Romero[1]*

Department of Pharmacology, Medical School, University of Minnesota, Minneapolis,[1] and Department of Biology, St. Olaf College, Northfield,[3] Minnesota, and Department of Medical Biochemistry and Genetics, Texas A&M University Health Science Center, College Station, Texas[2]

Received 3 December 2003/Accepted 23 June 2004

The ciliated protozoan *Tetrahymena thermophila* contains two distinct nuclei within a single cell—the mitotic micronucleus and the amitotic macronucleus. Although microtubules are required for proper division of both nuclei, macronuclear chromosomes lack centromeres and the role of microtubules in macronuclear division has not been established. Here we describe nuclear division defects in cells expressing a mutant β-tubulin allele that confers hypersensitivity to the microtubule-stabilizing drug paclitaxel. Macronuclear division is profoundly affected by the *btu1-1* (K350M) mutation, producing cells with widely variable DNA contents, including cells that lack macronuclei entirely. Protein expressed by the *btu1-1* allele is dominant over wild-type protein expressed by the *BTU2* locus. Normal macronuclear division is restored when the *btu1-1* allele is inactivated by targeted disruption or expressed as a truncated protein. Immunofluorescence studies reveal elongated microtubular structures that surround macronuclei that fail to migrate to the cleavage furrows. In contrast, other cytoplasmic microtubule-dependent processes, such as cytokinesis, cortical patterning, and oral apparatus assembly, appear to be unaffected in the mutant. Micronuclear division is also perturbed in the K350M mutant, producing nuclei with elongated early-anaphase spindle configurations that persist well after the initiation of cytokinesis. The K350M mutation affects tubulin dynamics, as the macronuclear division defect is exacerbated by three treatments that promote microtubule polymerization: (i) elevated temperatures, (ii) sublethal concentrations of paclitaxel, and (iii) high concentrations of dimethyl sulfoxide. Inhibition of phosphatidylinositol 3-kinase (PI 3-kinase) with 3-methyladenine or wortmannin also induces amacronucleate cell formation in a *btu1-1*-dependent manner. Conversely, the myosin light chain kinase inhibitor ML-7 has no effect on nuclear division in the *btu1-1* mutant strain. These findings provide new insights into microtubule dynamics and link the evolutionarily conserved PI 3-kinase signaling pathway to nuclear migration and/or division in *Tetrahymena*.

Microtubules are multifunctional cellular structures that mediate intracellular transport, cell motility, chromosome segregation, and cell division (40, 51). These polymers consist of noncovalently linked heterodimers of α- and β-tubulin that are decorated with microtubule-associated proteins that specify different biochemical and cellular properties (reviewed in reference 35). A critical event in chromosome transmission is the proper division and segregation of daughter nuclei. Astral microtubules that radiate from the spindle pole toward the cell cortex direct the migration of the mitotic nucleus prior to karyokinesis (reviewed in reference 32). This process is regulated by the concerted action of microtubule-dependent motors (kinesins and dyneins) and microtubule growth and shrinkage at the plus end. Actomyosin filaments generate the contractile ring filament at the cleavage furrow, and microtubules and septins complete cytokinesis (reference 43 and references therein).

The ciliated protozoan *Tetrahymena thermophila* has been used extensively as a model for studying microtubule-mediated cellular processes and deciphering the role of posttranslational modification of tubulin subunits (45). This research has been facilitated by the presence of a single α-tubulin gene (*ATU1*) and two β-tubulin genes (*BTU1* and *BTU2*) that encode identical proteins (19, 31). DNA transformation methodologies allow for the functional analysis of these genes by targeted homologous recombination. Cytological and biochemical studies have thus far identified at least 17 distinct types of microtubules with different subcellular localization patterns and/or associated proteins (16).

The role of microtubules in *Tetrahymena* nuclear division is likely to be complex, as *Tetrahymena* cells harbor two genetically related, but functionally distinct, nuclei—the germ line micronucleus and the somatic macronucleus (reviewed in reference 25). The transcriptionally silent diploid micronucleus serves as the reservoir of genetic information transmitted during conjugation and is thus dispensable for vegetative growth. The transcriptionally active polyploid macronucleus confers the cellular phenotypes during vegetative division and development. Microtubules play an essential role in mitotic and meiotic chromosome segregation in the diploid micronucleus. Furthermore, a meshlike microtubule network that forms at the conjugal junction facilitates the reciprocal exchange of pronuclei between mating cells (36).

* Corresponding author. Mailing address: Department of Pharmacology, Medical School, University of Minnesota, 6-120 Jackson Hall, 321 Church Street S.E., Minneapolis, MN 55455. Phone: (612) 624-8997. Fax: (612) 625-8408. E-mail: romero@med.umn.edu.

† J.J.S. and J.S.Y. contributed equally to this study.

‡ Present address: Biochemistry and Molecular Genetics, University of Virginia Health System, Charlottesville, VA 22908.

The contribution of microtubules to macronuclear division is less clear. Although intramacronuclear microtubules appear prior to karyokinesis, they are disordered (23). Since macronuclear chromosomes lack centromeres, sister chromatids segregate randomly (9) and spindle pole bodies do not form. Instead, a nonconventional yet ordered array of cytoplasmic microtubules assembles perpendicular to the division plane of the replicated macronucleus. The temporal reorganization of cytoplasmic microtubules suggests their involvement in macronuclear division. In support of this idea, abnormal macronuclear division can be induced with microtubule-destabilizing drugs such as colchicine (23, 44). The blockage of cell division in *Tetrahymena* by disruption of the kinesin-II gene (3) or by mutations that eliminate β-tubulin polyglycylation (45, 51) also implicates microtubules in cytokinesis.

Single amino acid substitutions in tubulin genes can dramatically alter microtubule stability. For example, the polymerization and stability of *Chlamydomonas reinhardtii* microtubules are enhanced by the β-tubulin K350M mutation, which imparts resistance to the microtubule-destabilizing drug vinblastine. This same mutation confers hypersensitivity to the microtubule-stabilizing drug paclitaxel (Taxol) (42). Similar drug sensitivities are observed in connection with the *T. thermophila btu1-1* (K350M) allele (18).

The *BTU1* locus has been exploited as a target site for introducing native or foreign genes that do not impart a selectable growth advantage on their own. Targeted disruption of the *btu1-1* (K350M) allele in strain CU522 confers resistance to the microtubule-stabilizing drug paclitaxel (17), making positive selection for transformants possible. In the course of experiments using the *btu1-1* locus for gene targeting, we uncovered cytogenetic evidence that microtubules are required for macronuclear division in vegetatively dividing *Tetrahymena*. We show that the *btu1-1* (K350M) allele acts in a dominant-negative manner to disrupt microtubule dynamics and decrease the fidelity of macronuclear transmission to daughter cells. We also provide in vivo evidence for the involvement of the signaling protein phosphatidylinositol 3-kinase (PI 3-kinase) in microtubule-mediated macronuclear division.

MATERIALS AND METHODS

General methods. Molecular techniques were performed as described elsewhere (1). *T. thermophila* genomic DNA was isolated by detergent lysis procedures as previously described (53). Total RNA was isolated from vegetative and conjugating cells by using RNeasy total RNA kits (QIAGEN, Valencia, Calif.). [^{32}P]-radiolabeled DNA probes were generated by PCR (30). Southern blotting and reverse transcriptase PCR (RT-PCR) analyses were performed as previously described (29).

***T. thermophila* strains and growth conditions.** *T. thermophila* strains CU522, CU725, and CU727 (Jacek Gaertig, University of Georgia) contain the mutant β-tubulin allele *btu1-1* (K350M), which confers hypersensitivity to paclitaxel. CU428 and SB1969 are wild-type strains, and TC219 is a spontaneous paclitaxel-resistant CU522 revertant. All strains were grown in 2% PPYS (PPYS is 2% proteose peptone, 0.2% yeast extract, 0.1% sequestrene) at 25, 30, and 35°C on a platform shaker as previously described (53). The potential role of microtubules and the PI 3-kinase signaling pathway in amacronucleate cell formation was examined by the addition of specific inhibitors to the culture media. Paclitaxel (1 mM stock in 100% ethanol; Sigma Chemicals) and vinblastine (0.5 mM stock in 50% ethanol; Sigma Chemicals) inhibited cell growth by ~50% at the final concentrations used (1 μM for paclitaxel and 5 μM for vinblastine). When used alone to study amacronucleate cell formation, dimethyl sulfoxide (DMSO) was added to a final concentration of 2%. Concentrations of 1.0% or less had no effect on amacronucleate cell formation. The PI 3-kinase inhibitor wortmannin (250 μM stock in 100% DMSO; Calbiochem) was diluted to a final concentration of 250 nM (the working concentration range in mammalian cell studies is 10 to 250 nM). The PI 3-kinase inhibitor 3-methyladenine (3-MA; 1 M stock in 100% DMSO; Sigma) was diluted to a final concentration of 10 mM (the working concentration in typical mammalian cell studies is 10 mM). The myosin light chain kinase (MLCK) inhibitor ML-7 (10 mM stock in 100% DMSO; Calbiochem) was diluted to a final concentration of 1 to 10 μM (the 50% inhibitory concentration is 300 nM for mammalian cells).

Transformation of *T. thermophila*. Strain CU522 was grown at 30°C in 100-ml cultures (2% PPYS) to a density of 1×10^5 to 3×10^5 cells/ml and starved in an equal volume of 10 mM Tris-HCl (pH 7.5) for 14 to 21 h. Cells were gently pelleted and resuspended in 1 to 3 ml of 10 mM HEPES (pH 7.5) to a density of approximately 10^7 cells/ml. The concentrated cells were transferred to a 100-mm-diameter petri dish that contained a sterile Whatman 114 filter paper presoaked with 2 ml of 10 mM HEPES (pH 7.5). The petri dish was placed in the Bio-Rad gene gun sample chamber, and gold particles (1.0 μm in diameter) coated with approximately 1.0 μg of a neomycin resistance cassette targeted to the *btu1-1* (K350M) locus (18) were introduced into cells biolistically as per the instructions of the manufacturer (Bio-Rad). After transformation, cells were incubated in 50 ml of prewarmed 2% PPYS at 30°C for 2 h. Paclitaxel was then added to the culture to a final concentration of 20 μM. Cells were distributed into 96-well plates (100-μl aliquots) and incubated in a dark humidity chamber at 30°C for 4 to 7 days. Clonal paclitaxel-resistant cell lines were screened by Southern blot analysis for disruption of the *btu1-1* (K350M) locus (29). Continuous selection in 20 to 40 μM paclitaxel was maintained until 100% phenotypic assortment relative to the disrupted allele was achieved, as confirmed by RT-PCR analysis of the targeted *btu1-1* (K350M) allele.

Cell synchronization and flow cytometry. Cell cycle synchronization was achieved by slight modification of a stationary-phase synchronization protocol described previously (34). Briefly, saturated cultures were starved for 8 h prior to dilution in growth media. Cells were stained with propidium iodide and monitored for synchronization by flow cytometry as previously described (7).

Feulgen staining and cytophotometry. Cells were grown to a density of 1×10^5 to 2×10^5 cells/ml prior to being harvested by centrifugation for Feulgen staining and dual-wavelength cytophotometry as previously described (28). Fifty individual micronuclei from conjugating pairs (CU428 × SB1969) were used as a reliable diploid (2N, 4C [where N is the number of chromosomes and 1C is the DNA content in a haploid nucleus]) standard to quantify the macronuclear DNA contents of vegetative dividing cells (10). The DNA contents of 50 and 200 macronuclei from vegetative CU428 and CU522 cultures, respectively, were determined for cells whose micronuclei were in early anaphase.

Confocal microscopy and immunofluorescence. One milliliter of a 10^5-cell/ml log-phase culture was fixed with 0.5 ml of Schaudinn's reagent as previously described (28). A single drop of VectraShield with 6-diamidino-2-phenylindole (DAPI; Vector Labs) was added to the cells prior to placement of 20 μl of the fixed cell suspension onto microscope slides. To obtain vegetative dividing cells for immunofluorescence analysis, 1 ml of a 10^5-cell/ml log-phase culture was fixed by the Triton-ethanol procedure (48). Basal bodies were visualized with a monoclonal primary antibody (FV4F9 diluted 1:20 in 1.0% bovine serum albumin [BSA] in Tris-buffered saline [TBS]) raised against a *Tetrahymena* basal body protein and fluorescein isothiocyanate-conjugated goat anti-mouse secondary antibody (diluted 1:100 in 1.0% BSA in TBS; Sigma Chemicals). Following fixation in paraformaldehyde (6), microtubules associated with *Tetrahymena* nuclei were visualized by using cross-reactivity with a monoclonal antibody specific for chicken α-tubulin (CPO6 diluted 1:100 in 1.0% BSA in TBS; Oncogene) as described previously (15). Nuclei were counterstained with Sytox (Molecular Probes) as previously described (6). Cells were examined either with conventional fluorescence microscopy with an Olympus B-Max fluorescence microscope at a magnification of ×320 by using a 40× oil immersion lens objective, a 1.6-optivar setting, and a 5× ocular lens objective or with a Bio-Rad MRC1000/1024 laser confocal microscope (University of Minnesota Imaging Center). Micrographs were recorded and images were overlaid using a SPOT camera and imaging software.

Acridine orange and Hoechst 33342 staining. Approximately 0.1 ml of cultured cells was doubly stained with Apofluor (0.001% acridine orange and 5 μg of Hoechst 33342/ml). Stained cells were immediately observed by fluorescence microscopy as described above.

Cell division and nuclear segregation analysis. Cells were fixed and stained with DAPI and visualized as previously described (28). Micrographs were recorded digitally using a SPOT camera and imaging software to create the negative images. Six micrograph images of each strain were captured, and the percentage of cells lacking macronuclei was recorded. Each strain was measured in three independent experiments when grown at 25, 30, or 35°C.

RESULTS

Targeting of the *btu1-1* (K350M) allele reveals a role for β-tubulin in macronuclear division. Drugs such as vinblastine and paclitaxel alter normal microtubule dynamics and are commonly used to block mitosis. A previous study of wild-type strains demonstrated that microtubule-inhibitory drugs interfere with amitotic macronuclear division in *T. thermophila* (20). In an effort to better understand the role of microtubules in both mitotic and amitotic nuclear division, we examined the fate of micro- and macronuclei in strains expressing either the wild-type (CU428) or paclitaxel-hypersensitive (CU522) β-tubulin allele *btu1-1* (K350M). In contrast to that in wild-type cells, macronuclear morphology in CU522 (*btu1-1*) cultures grown in the absence of paclitaxel showed significant variability, the most obvious differences being cells that had diminutive macronuclei or that lacked macronuclei entirely (Fig. 1A and B). Inactivation of the macronuclear *btu1-1* locus by targeted disruption with several unrelated transgenes restored wild-type macronuclear morphology and division (data not shown; see below), suggesting that the *btu1-1* mutation is responsible for the macronuclear division defect. Other *btu1-1* strains (CU725 and CU727) were similarly defective in macronuclear division.

Exacerbation of the *btu1-1* (K350M) amacronucleate phenotype at elevated temperatures. The *btu1-1* allele confers hypersensitivity to the microtubule-stabilizing drug paclitaxel. Since microtubules are also stabilized by elevated temperatures, we tested the effect of temperature on amacronucleate cell formation. Under standard culture conditions (30°C), ~6% of CU522 cells lacked macronuclei (Fig. 1B). The frequency of amacronucleate cell formation increased to ~12% when growing cultures were maintained at 35°C. In contrast, almost no amacronucleate cells were detected at 25°C. Irrespective of growth temperature, the amacronucleate phenotype was not detected in wild-type strain CU428, indicating that the temperature-sensitive effect is linked to the *btu1-1* allele.

Cytophotometric analysis revealed that the macronuclear DNA contents of cells expressing the *btu1-1* allele varied considerably compared to those of wild-type cells (Fig. 1C). When normalized to the postmeiotic 4C micronucleus, the average macronuclear DNA content of CU522 cells cultured at 35°C was 117C (standard error, ±66C; range, 31C to 546C). In contrast, the macronuclear DNA contents of wild-type CU428 cells grown under the same conditions were much more moderate (mean, 93C; standard error, ±13C; range, 64C to 132C), with values similar to those reported previously for wild-type *T. thermophila* strains (11). The wide range in macronuclear DNA contents in CU522 populations indicates that asymmetric macronuclear division occurs frequently. These events not only generate amacronucleate cells but also produce the reciprocal product of asymmetric macronuclear division—cells with an overabundance of macronuclear DNA.

The microtubule-stabilizing drugs paclitaxel and DMSO promote amacronucleate cell formation. The dominant *btu1-1* allele causes hypersensitivity to the microtubule-stabilizing agent paclitaxel. Since the nuclear division defect in the mutant is exacerbated at elevated temperatures, it seemed likely that microtubule dynamics were being affected at the higher temperatures. To test this hypothesis, we treated cells with increasing concentrations of drugs that stabilize (paclitaxel) or destabilize (vinblastine) microtubules. Titration curves were first generated for paclitaxel and vinblastine to identify drug concentrations that slowed down, but did not completely inhibit, cell growth (Fig. 2A and B). Drug concentrations that reduced the growth rate by ~50% were then tested for their effects on macronuclear division. Paclitaxel (1 μM) caused a sixfold increase in the frequency of amacronucleate CU522 cells (20% of the treated population), but 5 μM vinblastine had no effect (Fig. 2C).

DMSO has been shown to inhibit the polymerization of astral microtubules in *Xenopus laevis* egg extracts (41, 47). Two-percent DMSO produced a dramatic effect on amacro-

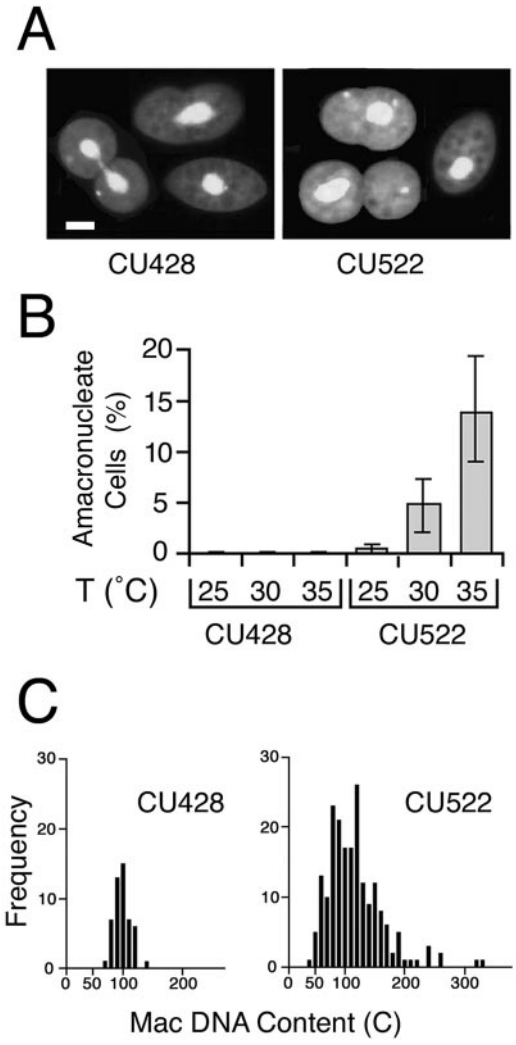

FIG. 1. *btu1-1* (K350M) expression is coincident with an amacronucleate phenotype. (A) Conventional fluorescent micrographs of Apofluor-stained wild-type *BTU1* and mutant *btu1-1* (K350M) strains (CU428 and CU522, respectively) grown at 35°C. Bar, 20 μm. (B) Percentages of amacronucleate cells in CU428 and CU522 cultures grown at 25, 30, and 35°C. Amacronucleate cells of each strain were quantified independently on three separate occasions, with an average of 600 cells scored for the amacronucleate phenotype per experiment. T, temperature. (C) Histograms showing the DNA contents for CU428 and CU522 cells. DNA contents were quantified cytophotometrically as previously described (10). Mac, macronuclear.

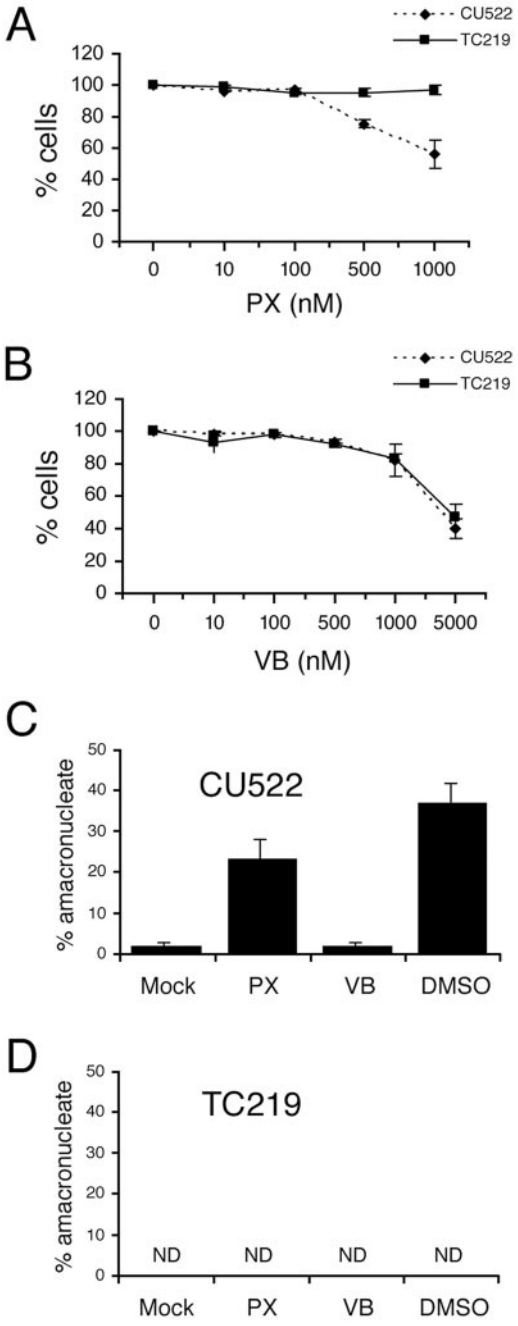

FIG. 2. Effect of paclitaxel, vinblastine, and DMSO on CU522 (*btu1-1*) and TC219 revertant cells. (A and B) Dose-dependent effects of paclitaxel (PX) and vinblastine (VB) on growth of CU522 and TC219 cells. Vegetative cells were cultured overnight in different concentrations of microtubule polymerization (paclitaxel) or depolymerization (vinblastine) inhibitors, and cell densities were determined with a hemocytometer. (C and D) Effects of microtubule inhibitors on amacronucleate cell formation. Vegetative cells (CU522 and TC219) were treated for 9 h with 1 μM paclitaxel, 5 μM vinblastine, or 2% DMSO. The percentages of amacronucleate cells were determined by fluorescence microcopy of DAPI-treated cells. Data are the means ± standard deviations of results from three experiments in which 200 cells per sample were counted. ND, no amacronucleate cells detected.

nucleate cell formation: more than one-third of the CU522 cell population lacked a macronucleus (Fig. 2C). The titration curve for DMSO was steep, as 1% DMSO had virtually no effect on amacronucleate cell formation and 4% DMSO was toxic (data not shown). Remarkably, cells with two macronuclei were not detected in all populations treated with regimens that enhanced amacronucleate cell formation (exposure to elevated temperatures, paclitaxel, and DMSO). Similar to elevated temperatures, microtubule-stabilizing drugs had no effect on macronuclear division in cells expressing just the full-length wild-type β-tubulin gene (Fig. 2D shows data for TC219, a CU522 revertant; see below). The allele-specific effect of DMSO and paclitaxel suggests that both drugs target *Tetrahymena* microtubules in vivo.

Paclitaxel resistance correlates with the loss of the amacronucleate phenotype. As noted above, disruption of the *btu1-1* (K350M) allele by insertion of a foreign gene confers paclitaxel resistance. During the selection for targeted *btu1-1* transformants, nontransformed clonal lines resistant to paclitaxel were also isolated. RT-PCR analysis of mRNA from one of these spontaneous mutant strains (TC219) revealed wild-type levels of *btu1-1* mRNA expression (Fig. 3A). TC219 and an independently isolated *btu1-1*::Neo transformant failed to produce the amacronucleate phenotype at all tested growth temperatures (Fig. 3B). Sequence analysis of *btu1-1* cDNA from TC219 revealed a 4-bp deletion at the β-tubulin codon corresponding to S339, resulting in missense translation of *btu1-1* until a nonsense codon was encountered 76 codons beyond the S339 codon (Fig. 3C). Thus, the loss of the amacronucleate phenotype when the *btu1-1* allele is either disrupted or mutated demonstrates that expression of the β-tubulin K350M mutation is responsible for the macronuclear division defect. Since the CU522 strain also expresses wild-type β-tubulin from the *BTU2* locus, the mutant *btu1-1* (K350M) allele must be dominant over the wild type.

***btu1-1* (K350M) nuclear phenotypes.** CU522 and TC219 strains were examined by conventional and confocal microscopy to assess the organization of microtubules at various stages of cell division. A panel of confocal images clearly illustrates that the amacronucleate phenotype in CU522 results from a delay or failure in macronuclear elongation and division (Fig. 4A). Although the micronuclei in dividing CU522 cells often exhibit the normal round and condensed shape seen in wild-type cells during cytokinesis, a large percentage of cells possessed micronuclei with an elongated spindle shape characteristic of micronuclear anaphase (Fig. 4B). This apparent delay in micronuclear division was detected only in cells expressing the *btu1-1* (K350M) allele.

Nuclear microtubules were visualized directly with a monoclonal antibody that cross-reacts with *Tetrahymena* α-tubulin. Confocal immunofluorescence images of dividing CU522 and TC219 cells are shown in Fig. 5. Three observations were immediately apparent. First, abnormally long microtubule bundles were detected early in cell division as spiraling whorls that encircled macronuclei in CU522 cells but not in TC219 cells (Fig. 5B, C, and E). These structures were reminiscent of those described by Fujiu and Numata (15) for wild-type *Tetrahymena* cells whose macronuclear microtubules had been stabilized artificially with high concentrations of paclitaxel. Second, immediately preceding cytokinesis, unusually robust

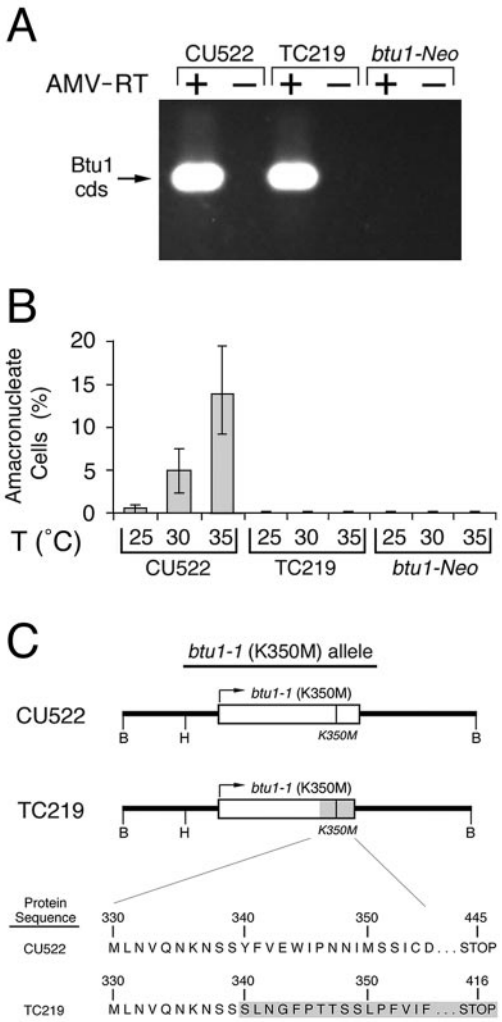

FIG. 3. A spontaneous mutation at the *btu1-1* locus leads to paclitaxel resistance. (A) RT-PCR analysis of total RNA (2 μg) from CU522 (paclitaxel sensitive), TC219 (paclitaxel resistant), and *btu1-1*::Neo (a paclitaxel-resistant transformant whose *btu1-1* locus has been disrupted by the neomycin resistance cassette) with primers specific for the *btu1-1* locus. An ethidium bromide-stained agarose gel of the RT-PCR products (with [+] or without [−] avian myeloblastosis virus RT [AMV-RT]) is shown. cds, coding sequence. (B) The percentages of amacronucleate cells at 25, 30, and 35°C for CU522 (paclitaxel sensitive), TC219 (paclitaxel resistant), and *btu1-1*::Neo (paclitaxel resistant) were quantified as described for Fig. 1B. T, temperature. (C) Partial open reading frames for the *btu1-1* alleles from the paclitaxel-sensitive strain CU522 and the paclitaxel-resistant strain TC219 are shown. The shaded area for the TC219 *btu1-1* allele represents the region downstream of codon 340 that is frame shifted due to a spontaneous 4-bp deletion. B and H, recognition sites for BamHI and HindIII, respectively.

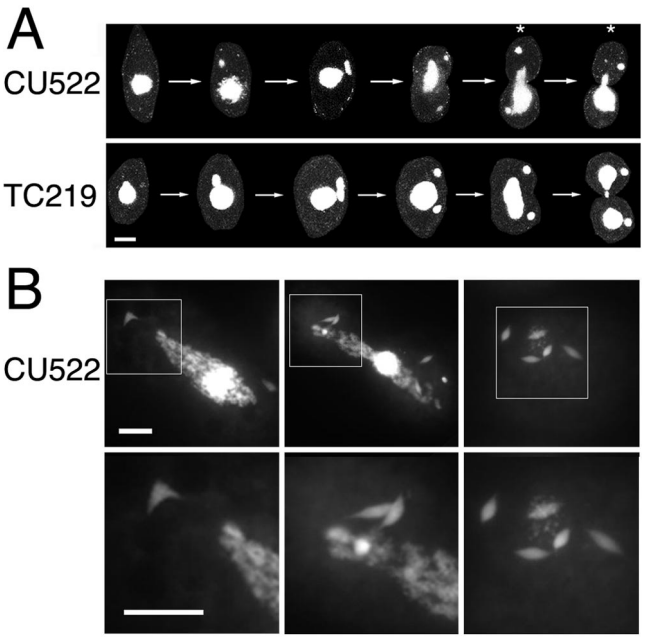

FIG. 4. Abnormal nuclear morphologies of dividing cells that express β-tubulin K350M. (A) Confocal images of representative CU522 and TC219 cells stained with DAPI at different stages of the cell cycle. The asterisks mark the unequal segregation of the macronucleus during cytokinesis in strain CU522. (B) Conventional fluorescence microscopy of DAPI-stained CU522 cells grown at 35°C. In the more highly magnified images (lower panels, corresponding to the boxed regions in the upper panels), micronuclei with elongated mitotic spindles that persist well beyond the initiation of cytokinesis are evident. Bars, 20 μm.

bundles of microtubules were associated with the macronuclei. The abnormally elongated macronuclei often failed to form macronuclear constrictions (compare Fig. 5D and F). The microtubule bundles occasionally wrapped around inside one of the two daughters in cells that failed to undergo macronuclear division (Fig. 5H). A third, less conspicuous phenotype was the persistence of micronuclei in an elongate, early-anaphase spindle configuration (Fig. 5). These structures were present long after micronuclear division was completed in strain TC219 (data not shown). The micronuclei often segregated wholly with one or the other future daughter (Fig. 5H) and as a result would be expected to generate both multimicronucleate and amicronucleate cells.

For the three paclitaxel-sensitive strains tested (CU522, CU725, and CU727), careful cytological examination failed to uncover any defects in cytokinesis, such as mislocalization of the cleavage furrow (data not shown). To more completely assess whether the *btu1-1* (K350M) mutation affects nonnuclear microtubule-mediated processes, we examined the structure and propagation of the oral apparatus and cortical patterning in paclitaxel-resistant (TC219) and -sensitive (CU522) strains (Fig. 6). Representative images of TC219 were indistinguishable from those of CU522. Immunocytochemical staining with polyclonal antisera specific for *Tetrahymena* basal bodies (5) revealed normal oral and cortical development during cell division (Fig. 6F to K). Fission furrows and oral primordia were evident in cells that contained small macronuclei or no macronuclei at all. Cortical development was similarly unaffected. Consistent with the observed defect in macronuclear transmission (Fig. 1A and Fig. 4), the macronuclei were unequally positioned across the cleavage furrows during cytokinesis in many CU522 cells (Fig. 6F to J). In contrast, the elongated macronuclei were evenly distributed across the cleavage furrows in TC219 revertants (Fig. 6A to D). Thus, asymmetric positioning of the replicated macronuclei

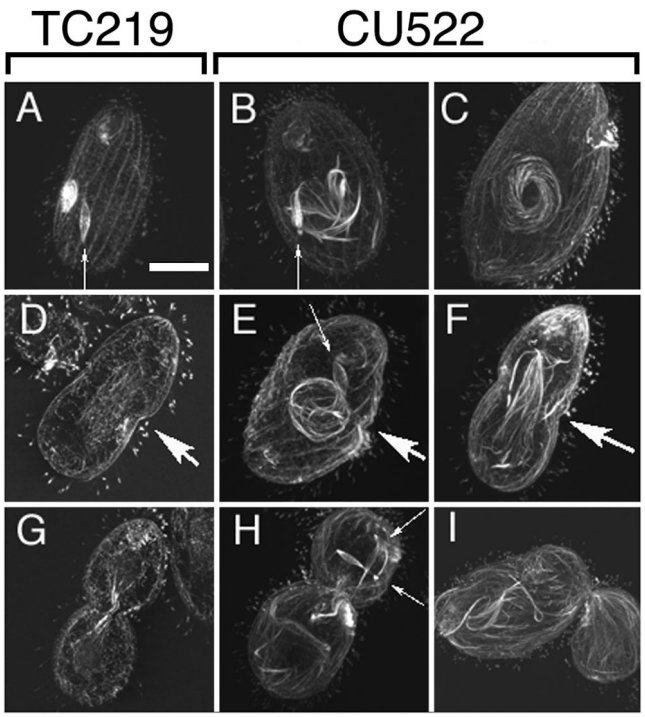

FIG. 5. Immunocytological analysis of microtubules associated with nuclei in strains CU522 and TC219. Confocal fluorescent images of paclitaxel-resistant TC219 cells (A, D, and G) and paclitaxel-hypersensitive CU522 cells (B, C, E, F, H, and I) are shown. Vegetatively dividing cells were maintained at 35°C prior to fixation and labeling with an antibody specific for α-tubulin (CPO6; Oncogene). (A to C) Cells in the first row are representative of those in the early stages of cell division, just prior to macronuclear division stage 1 (15) and at oral development stages 2 to 4 (14). (D to F) Cells in the second row represent those that have initiated cytokinesis and macronuclear division stages 2 to 3. (G to I) The third row represents cells near the completion of cytokinesis and macronuclear development stages 5 to 6 (15). Large arrows indicate the developing cleavage furrows, whereas small arrows point to micronuclear spindles. Bar, 20 μm.

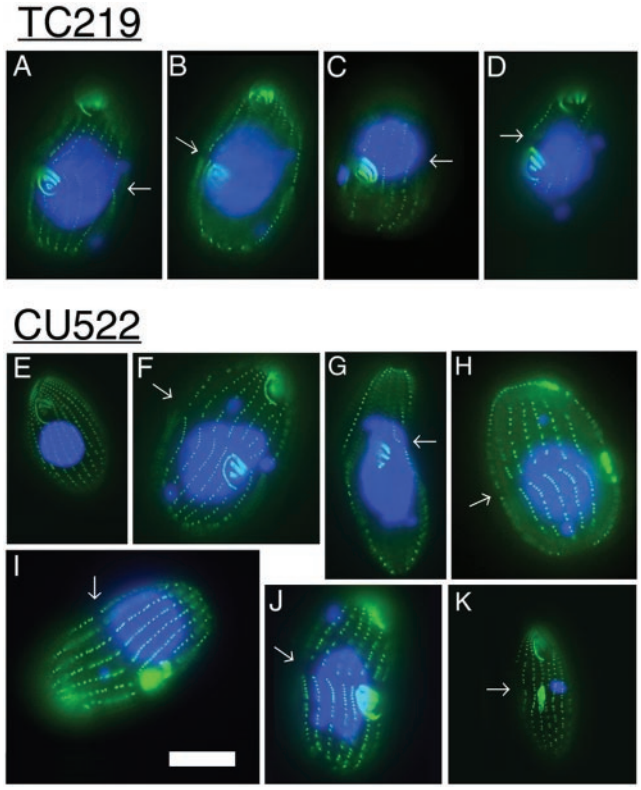

FIG. 6. Immunocytological analysis of cell membrane-associated microtubule-containing compartments in vegetatively dividing strains CU522 and TC219. Shown are fluorescent images of cells grown as described for Fig. 5 prior to fixation and labeling with FV4F9, a polyclonal antibody specific for basal body antigens (fluorescein isothiocyanate), and counterstained with DAPI (blue). Images in panels A to D are of TC219 cells, which do not express full-length K350M β-tubulin. Images in panels E to K are of CU522 cells, which express K350M β-tubulin and are hypersensitive to paclitaxel. The fission furrows formed during the initiation of cytokinesis are marked with arrows. Note the pattern of membrane-associated microtubule structures: basal bodies are along ciliary rows, apical (parental) oral apparatus, and medial (daughter) oral primordia. The indistinguishable pattern in these two strains suggests that the K350M mutation has no effect on basal body- or oral apparatus-associated microtubules (see the text for discussion). Bar, 20 μm.

may possibly account for the wide variation in macronuclear DNA contents in CU522 cell populations (Fig. 1C).

PI 3-kinase inhibitors exacerbate the macronuclear division defect in the *btu1-1* mutant. PI 3-kinase activates intracellular signaling cascades that are important for the regulation of many metabolic events in the cell cycle (4). The p55 and p85 regulatory subunits of mammalian PI 3-kinase bind to β-tubulin in vitro and exhibit perinuclear staining in vivo (22, 24). Although enzymatic evidence for PI 3-kinase has not yet been obtained for *Tetrahymena*, biochemical studies have identified the substrate for PI 3-kinase, PIP2 (phosphatidylinositol 4,5 diphosphate) (26, 27, 52). In addition, the PI 3-kinase inhibitors wortmannin and 3-MA inhibit caspase-induced autophagy (52), similar to their well-documented effects on mammalian cells and the slime mold *Dictyostelium discoideum* (38).

BLAST analysis of the unannotated *T. thermophila* genome database (http://www.tigr.org/tdb/e2k1/ttg/) revealed several strong candidate orthologues of the PI 3-kinase catalytic subunit. The most conserved homology was found in a 357-kb *Tetrahymena* genome scaffold (no. 8254435) within six predicted exons that span ~60% of the human catalytic subunit coding region. When the combined exons were used to query the National Center for Biotechnology Information nonredundant sequence database, strong homology was observed with the PI 3-kinase catalytic subunits from a wide variety of eukaryotes, including the slime mold *D. discoideum* (expected [E] value, 2^{-76}) and vertebrates (*Homo sapiens*; E value, 3^{-63}) (Fig. 7A). Similar searches identified a strong *Tetrahymena* candidate for the phosphatase and tensin homologue (PTEN), the enzyme that reverses the reaction catalyzed by PI 3-kinase (Fig. 7B). These data indicate that *Tetrahymena* encodes the key components of the classical PI 3-kinase pathway.

Since mammalian PI 3-kinase associates with β-tubulin, we asked whether *Tetrahymena* PI 3-kinase was involved in microtubule-mediated macronuclear division. *Tetrahymena* strains CU428 (*BTU1*) and CU522 (*btu1-1*) and the spontaneous revertant TC219 were treated with the PI 3-kinase inhibitors wortmannin and 3-MA at concentrations similar to those used

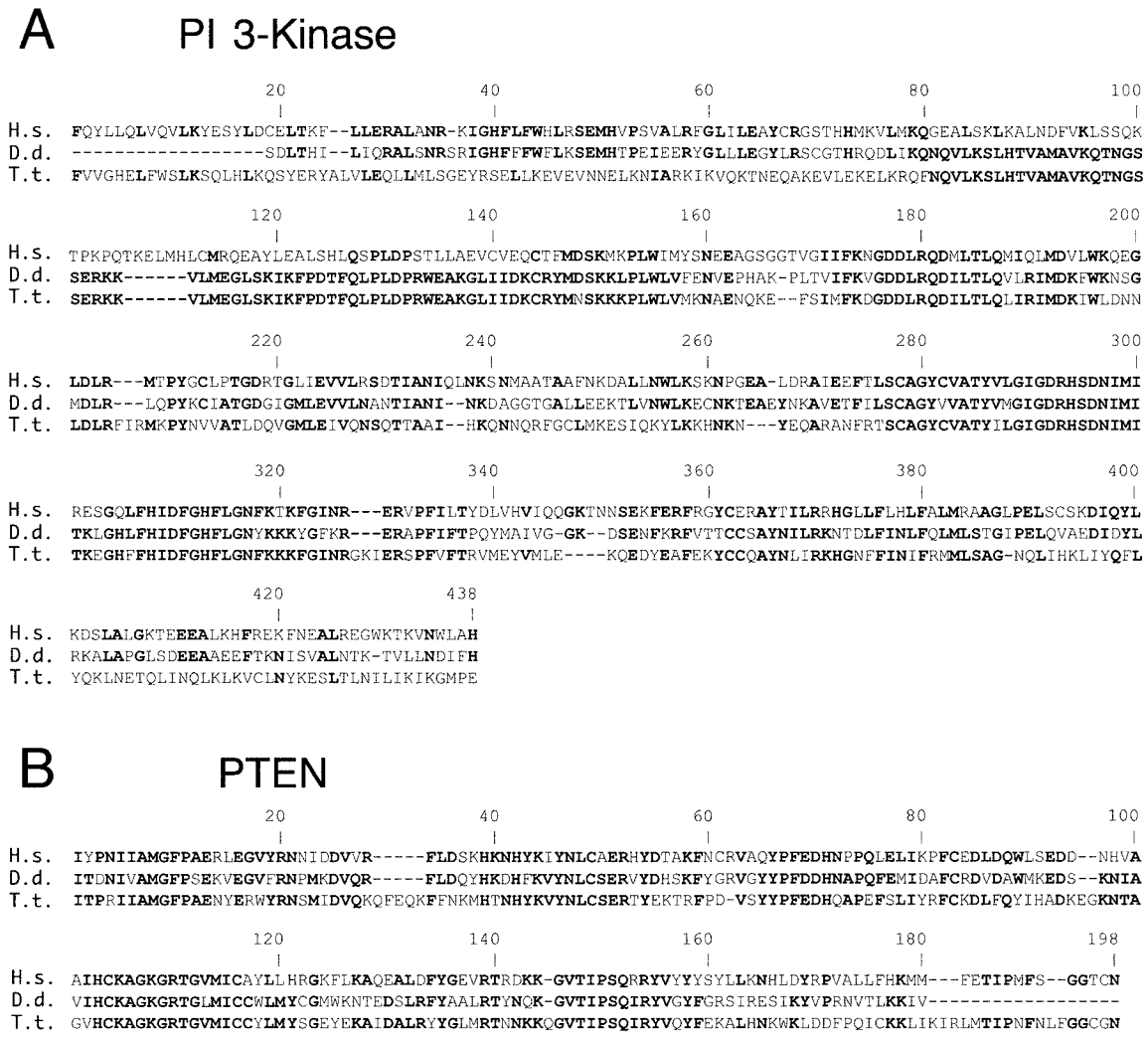

FIG. 7. Candidate *Tetrahymena* orthologues of the PI 3-kinase catalytic subunit and PTEN. Shown are MULTALIN multiple sequence alignments of human (*H.s.*) PI 3-kinase (A) and PTEN (B) with conserved protein domains in the translated *D. discoideum* (*D.d.*) and *T. thermophila* (*T.t.*) genome databases. Boldfaced amino acids are shared between at least two of the depicted species. The strongest *Tetrahymena* PI 3-kinase catalytic subunit and PTEN candidate genes reside on *Tetrahymena* sequence scaffolds 8254435 and 8254807, respectively (http://www.tigr.org/tdb/e2k1/ttg/). BLAST analysis E values obtained using the *Tetrahymena* PI 3-kinase catalytic subunit candidate gene as the query were 2^{-76} for the *D. discoideum* PI 3-kinase subunit gene (GenBank accession no. U23477.1) and 3^{-63} for the human PI 3-kinase subunit gene (GenBank accession no. U57843.1). E values obtained with the *Tetrahymena* PTEN candidate gene query were 2^{-43} for the *D. discoideum* PTEN gene (GenBank accession no. AF467431.1) and 8^{-42} for the human PTEN gene (GenBank accession no. U92436.1).

in mammalian cell studies (13, 33, 39). When these drugs were added to synchronized cells at various times following release from G_0/G_1 arrest, a significant increase in the frequency of amacronucleate cell formation was observed (Fig. 8A). This effect was limited to the β-tubulin K350M mutant alone and was most pronounced when inhibitors were added to S/G_2-phase cells. Thus, the effect of PI 3-kinase inhibitors on macronuclear division was dependent on expression of the *btu1-1* (K350M) allele.

Since high concentrations of wortmannin inhibit mammalian MLCK (46) and an unusual myosin-like protein is required for macronuclear elongation in *Tetrahymena* (50), we asked whether the highly specific MLCK inhibitor ML-7 could also induce amacronucleate cell formation. ML-7 at concentrations of 1 to 10 μM (50% inhibitory concentration for mammalian cells, 300 nM) had no effect on macronuclear division (data not shown). Higher concentrations of ML-7 (50 to 100 μM) were toxic and therefore uninformative.

Flow cytometry was used to examine the effect of 3-MA on cell cycle progression in CU522 cells. A partial block in the cell cycle was observed when the drug was added to G_0-arrested and refed cells (Fig. 8B; compare panels for 3 h after refeeding). There was significant accumulation of cells with lower than normal DNA contents 6 h after drug treatment (sub-G_0 peak), most likely due to the asymmetric macronuclear division documented for this strain. The sub-G_0 peak was more pronounced when 3-MA was added to cultures that were predominantly in the S/G_2 stage of the cell cycle (Fig. 8B, lower panels). This observation is consistent with the increased frequency of amacronucleate cell formation documented micro-

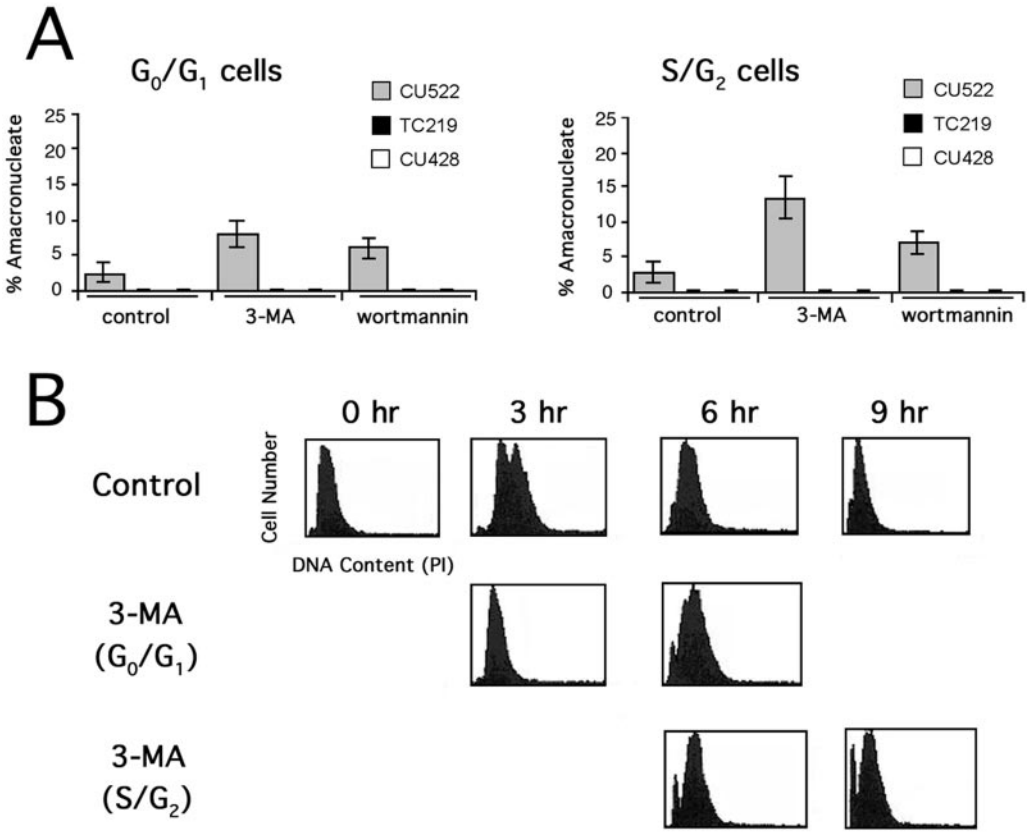

FIG. 8. PI 3-kinase inhibitors exacerbate the amacronucleate phenotype in CU522 cells and partially arrest cells at the G_1/S boundary. Ten-micromolar 3-MA or 250 nM wortmannin was added to synchronized vegetative cultures (strains CU522, TC219, and CU428) during G_0/G_1 or S/G_2. (A) The percentages of amacronucleate cells were determined by fluorescence microscopy following a 6-h incubation with or without drug treatment. (B) Results of flow cytometry analysis of synchronized CU522 cultures 0, 3, 6, and 9 h after addition of 3-MA. A measure of the relative DNA contents (abscissas) indicates arrest of a subpopulation at the G_1/S boundary and formation of a sub-G_0 peak (indicative of asymmetric macronuclear division) when 3-MA was added during G_0/G_1. The sub-G_0 peak was more pronounced when 3-MA was added during S/G_2.

scopically (Fig. 8A). Since the PI 3-kinase inhibitors produced the same effect on macronuclear segregation as three known treatments that stabilize microtubules, we conclude that the PI 3-kinase pathway is required for proper macronuclear division. The dependence of PI 3-kinase inhibitors on the *btu1-1* (K350M) mutation suggests that this kinase regulates microtubule-mediated processes that are dedicated to nuclear division.

DISCUSSION

Previous cytological studies provide a framework for the events associated with macronuclear division (23, 44). Upon completion of micronuclear mitosis, the macronucleus aligns at the cleavage furrow and divides more or less equally prior to cytokinesis. Cytoplasmic microtubules associate with the macronucleus in large numbers at this time, often forming bundles at the beginning of the elongation phase. These bundles ultimately localize to the constricted center of the bilobed dividing macronucleus. Macronuclear division and segregation typically precede the formation of a pronounced cytoplasmic cleavage furrow. Colchicine and other microtubule polymerization inhibitors block macronuclear constriction and disrupt the temporal relationship between macronuclear division and cytokinesis, often resulting in two daughter cells that receive grossly unequal quantities of nuclear material. It has been suggested that macronuclear division under these circumstances is mediated by pressure exerted by the cleavage furrow (23, 49). Since the macronuclear division defect observed in the *btu1-1* mutant is strikingly similar to that described for colchicine-treated wild-type cells, this process must be regulated by dynamic changes in microtubule polymerization and depolymerization. This prediction is borne out by our observation that three regimens that stabilize microtubule polymerization (elevated temperatures, high DMSO concentrations, and sublethal concentrations of paclitaxel) increase amacronucleate cell formation in the *btu1-1* mutant.

Since amitotic macronuclear division is inherently imprecise, variation in macronuclear DNA contents occurs naturally in wild-type *Tetrahymena* populations. Unconventional mechanisms have evolved to maintain genic balance. For example, excess macronuclear DNA is eliminated from the macronucleus in the form of chromosome extrusion bodies (2). When DNA content drops below a threshold, the macronucleus undergoes an endoreplication cycle prior to cell division (10). The broadened macronuclear DNA content profile of CU522 cells is best explained by a failure in macronuclear division rather

than replication, since cells with higher and lower than normal DNA contents were observed. Thus, the two extremes in the population (cells with abnormally high DNA contents and those with no macronuclei at all) represent failures in macronuclear migration and/or division.

Despite the fundamental differences in micro- and macronuclear division (mitotic versus amitotic), expression of *btu1-1* (K350M) impacts both processes. Since cytokinesis, cortical patterning, and oral apparatus assembly appear to be unaffected, the *btu1-1* allele behaves like a separation-of-function mutation. Microtubule stability is enhanced by this mutation, resulting in hypersensitivity to paclitaxel and distinct aberrations in nuclear-associated microtubules. During the early stages of cell division, CU522 cells grown at 35°C exhibit pronounced macronuclear microtubules in a spiral array (Fig. 5) that closely resemble those detected in wild-type cells treated with paclitaxel (15). Coincident with the first stages of cytokinesis, macronuclear microtubules accumulate in strange and persistent bipolar spindles. The appearance of these unusually robust microtubule bundles correlates with the failure in macronuclear division. In contrast, persistent microtubule spindles are associated with the mitotic micronuclear chromosomes during anaphase. These spindles are normally absent well before macronuclear elongation and the initiation of cytokinesis (Fig. 5). Taken together, it is likely that the enhanced stability of microtubules that have incorporated β-tubulin K350M alters normal microtubule dynamics, leading to the nuclear phenotypes described in this study.

In *Saccharomyces cerevisiae* and fungi, astral microtubules that emanate from the spindle pole body scan the mother cell cortex and direct the migration of the mitotic nucleus to the cleavage furrow. When nuclear migration is blocked, the nucleus still divides, thereby generating a binucleate and an anucleate daughter (reference 1a and references therein). Remarkably, cells with two (or more) macronuclei were not observed, suggesting that macronuclear division does not occur in missegregation mutants. Since the *Tetrahymena* macronucleus lacks a spindle pole body, the mechanism for macronuclear segregation must be inherently unique. Whether macronuclear migration is required for division is not known. Current data cannot rule out the possibility that the macronuclear division defect in the *btu1-1* mutant is due solely to a defect in nuclear migration.

Recent studies have demonstrated a role for structural (actin and tubulin) and motor (myosin and kinesin) proteins in macronuclear division and cytokinesis in *Tetrahymena*. In contrast to the *btu1-1* (K350M) allele described here, mutations documented for these proteins affect nuclear and cytoskeletal processes. For example, deletion of the *MYO1* gene, which encodes an unusual myosin-like protein, causes defects in endocytosis and macronuclear division (50). Similarly, expression of green fluorescent protein-tagged actin blocks macronuclear division and cytokinesis (20). Thus, both actomyosin filaments (20, 50) and cytoplasmic microtubules (this work) are required for proper macronuclear division. Whether the β-tubulin K350M mutation disrupts an interaction between cytoplasmic microtubules and actomyosin filaments remains to be determined.

It is also possible that the increase in microtubule stability and the associated macronuclear division defect may be mediated by the net loss of a positive charge in β-tubulin K350M. Alternatively, the K350M substitution may block posttranslational modification of K350 or nearby residues. Since the K350M mutation is dominant over the wild type, this mutation may affect the integrity of mixed microtubule polymers. Consistent with this prediction, the deduced β-tubulin product in the TC219 revertant strain lacks the domain(s) at the β-tubulin C terminus required for microtubule assembly (12). Consequently, the truncated protein would not be expected to contribute to microtubule-related functions. The simultaneous loss of the amacronucleate phenotype and reacquisition of paclitaxel resistance support this contention.

The pharmacological studies presented here suggest a novel role for the PI signaling pathway in macronuclear division. Specific inhibitors of PI 3-kinase induce asymmetric macronuclear division and amacronucleate cell formation. These agents effectively amplify the nuclear division defect of the β-tubulin K350M mutant in a manner analogous to those of previously established treatments that enhance microtubule stability (elevated temperatures, high DMSO concentrations, and sublethal concentrations of paclitaxel). Furthermore, the PI 3-kinase inhibitors showed no evidence of general cytotoxicity at the concentrations used, and other cytotoxic drugs that target microtubules or actomyosin filaments showed no effect on macronuclear division. Additional studies are needed to determine the exact relationship of the PI 3-kinase signaling pathway to macronuclear division. In vitro mammalian studies have demonstrated interactions between the regulatory subunits of PI 3-kinase and α-, β-, and γ-tubulins (24), and PI 3-kinase inhibitors increase the efficacy of paclitaxel in ovarian cancer models (21). Since several distinct point mutations in the β-tubulin gene (not the K350M mutation) can lead to clinical drug resistance (reviewed in reference 37), a better understanding of how PI 3-kinase regulates microtubule dynamics in the genetically tractable eukaryote *Tetrahymena* may provide new insights. Recent studies in plants have identified another phospholipid signaling enzyme, phospholipase D, that interacts with microtubules in vivo and mediates stress-induced microtubule reorganization (8). Our demonstration of a functional in vivo link between β-tubulin and PI 3-kinase in *Tetrahymena* suggests a concerted role for these proteins in the regulation of nuclear division.

ACKNOWLEDGMENTS

This work was supported by NSF grant MCB 0220085 (D.P.R.), NIH grant GM53572 (G.M.K.), and NSF RUI grant MCB 0131175 (E.S.C.).

We thank Dorothy Shippen for careful reading of the manuscript and valuable comments.

REFERENCES

1. **Ausubel, F. M., et al. (ed.).** 2004. Current protocols in molecular biology. [Online.] John Wiley and Sons, Inc., Hoboken, N.J. http://www.mrw.interscience.wiley.com/cp/cpmb/cpmb_contents_fs.html.

1a. **Beach, D. L., J. Thibodeaux, P. Maddox, E. Yeh, and K. Bloom.** 2000. The role of the proteins Kar9 and Myo2 in orienting the mitotic spindle of budding yeast. Curr. Biol. **10:**1497–1506.

2. **Bodenbender, J., A. Prohaska, F. Jauker, H. Hipke, and G. Cleffmann.** 1992. DNA elimination and its relation to quantities in the macronucleus of *Tetrahymena*. Dev. Genet. **13:**103–110.

3. **Brown, J. M., C. Marsala, R. Kosoy, and J. Gaertig.** 1999. Kinesin-II is preferentially targeted to assembling cilia and is required for ciliogenesis and normal cytokinesis in *Tetrahymena*. Mol. Biol. Cell **10:**3081–3096.

4. **Chang, F., J. T. Lee, P. M. Navolanic, L. S. Steelman, J. G. Shelton, W. L.**

Blalock, R. A. Franklin, and J. A. McCubrey. 2003. Involvement of PI3K/Akt pathway in cell cycle progression, apoptosis, and neoplastic transformation: a target for cancer chemotherapy. Leukemia **17:**590–603.
5. **Cole, E. S., and J. Frankel.** 1991. Conjugal blocks in *Tetrahymena* pattern mutants and their cytoplasmic rescue. II. Janus A. Dev. Biol. **148:**420–428.
6. **Cole, E. S., K. R. Stuart, T. C. Marsh, K. Aufderheide, and W. Ringlien.** 2002. Confocal fluorescence microscopy for *Tetrahymena thermophila*. Methods Cell Biol. **70:**337–359.
7. **Darzynkiewicz, Z., G. Juan, and E. Bedner.** 2004. Determining cell cycle stages by flow cytometry. Current protocols in cell biology, section 8.4. [Online.] John Wiley and Sons, Inc., Hoboken, N.J. http://www.mrw.interscience.wiley.com/cp/cpcb/articles/cb0804/frame.html.
8. **Dhonukshe, P., A. M. Laxalt, J. Goedhart, T. W. Gadella, and T. Munnik.** 2003. Phospholipase D activation correlates with microtubule reorganization in living plant cells. Plant Cell **15:**2666–2679.
9. **Doerder, F. P.** 1979. Regulation of macronuclear DNA content in *Tetrahymena thermophila*. J. Protozool. **26:**28–35.
10. **Doerder, F. P., and L. E. Debault.** 1975. Cytofluorimetric analysis of nuclear DNA during meiosis, fertilization and macronuclear development in the ciliate *Tetrahymena pyriformis*, syngen 1. J. Cell Sci. **17:**471–493.
11. **Doerder, F. P., and L. E. DeBault.** 1978. Life cycle variation and regulation of macronuclear DNA content in *Tetrahymena thermophila*. Chromosoma **69:**1–19.
12. **Duan, J., and M. A. Gorovsky.** 2002. Both carboxy-terminal tails of α- and β-tubulin are essential, but either one will suffice. Curr. Biol. **12:**313–316.
13. **Eskelinen, E. L., A. R. Prescott, J. Cooper, S. M. Brachmann, L. Wang, X. Tang, J. M. Backer, and J. M. Lucocq.** 2002. Inhibition of autophagy in mitotic animal cells. Traffic **3:**878–893.
14. **Frankel, J., and E. M. Nelsen.** 2001. The effects of supraoptimal temperatures on population growth and cortical patterning in *Tetrahymena pyriformis* and *Tetrahymena thermophila*: a comparison. J. Eukaryot. Microbiol. **48:**135–146.
15. **Fujiu, K., and O. Numata.** 2000. Reorganization of microtubules in the amitotically dividing macronucleus of *Tetrahymena*. Cell Motil. Cytoskelet. **46:**17–27.
16. **Gaertig, J.** 2000. Molecular mechanisms of microtubular organelle assembly in *Tetrahymena*. J. Eukaryot. Microbiol. **47:**185–190.
17. **Gaertig, J., Y. Gao, T. Tishgarten, T. G. Clark, and H. W. Dickerson.** 1999. Surface display of a parasite antigen in the ciliate *Tetrahymena thermophila*. Nat. Biotechnol. **17:**462–465.
18. **Gaertig, J., T. H. Thatcher, L. Gu, and M. A. Gorovsky.** 1994. Electroporation-mediated replacement of a positively and negatively selectable β-tubulin gene in *Tetrahymena thermophila*. Proc. Natl. Acad. Sci. USA **91:**4549–4553.
19. **Gaertig, J., T. H. Thatcher, K. E. McGrath, R. C. Callahan, and M. A. Gorovsky.** 1993. Perspectives on tubulin isotype function and evolution based on the observation that *Tetrahymena thermophila* microtubules contain a single α- and β-tubulin. Cell Motil. Cytoskelet. **25:**243–253.
20. **Hosein, R. E., S. A. Williams, K. Haye, and R. H. Gavin.** 2003. Expression of GFP-actin leads to failure of nuclear elongation and cytokinesis in *Tetrahymena thermophila*. J. Eukaryot. Microbiol. **50:**403–408.
21. **Hu, L., J. Hofmann, Y. Lu, G. B. Mills, and R. B. Jaffe.** 2002. Inhibition of phosphatidylinositol 3′-kinase increases efficacy of paclitaxel in *in vitro* and *in vivo* ovarian cancer models. Cancer Res. **62:**1087–1092.
22. **Inukai, K., M. Funaki, M. Nawano, H. Katagiri, T. Ogihara, M. Anai, Y. Onishi, H. Sakoda, H. Ono, Y. Fukushima, M. Kikuchi, Y. Oka, and T. Asano.** 2000. The N-terminal 34 residues of the 55 kDa regulatory subunits of phosphoinositide 3-kinase interact with tubulin. Biochem. J. **346:**483–489.
23. **Jaeckel-Williams, R.** 1978. Nuclear divisions with reduced numbers of microtubules in *Tetrahymena*. J. Cell Sci. **34:**303–319.
24. **Kapeller, R., A. Toker, L. C. Cantley, and C. L. Carpenter.** 1995. Phosphoinositide 3-kinase binds constitutively to α/β-tubulin and binds to γ-tubulin in response to insulin. J. Biol. Chem. **270:**25985–25991.
25. **Karrer, K. M.** 2000. *Tetrahymena* genetics: two nuclei are better than one. Methods Cell Biol. **62:**127–186.
26. **Kovacs, P., and G. Csaba.** 1990. Involvement of the phosphoinositol (PI) system in the mechanism of hormonal imprinting. Biochem. Biophys. Res. Commun. **170:**119–126.
27. **Kovacs, P., and E. Pallinger.** 2003. Effects of indomethacin on the divisional morphogenesis and cytoskeleton-dependent processes of *Tetrahymena*. Cell Biochem. Funct. **21:**169–175.
28. **Marsh, T. C., E. S. Cole, and D. P. Romero.** 2001. The transition from conjugal development to the first vegetative cell division is dependent on *RAD51* expression in the ciliate *Tetrahymena thermophila*. Genetics **157:**1591–1598.
29. **Marsh, T. C., E. S. Cole, K. R. Stuart, C. Campbell, and D. P. Romero.** 2000. *RAD51* is required for propagation of the germinal nucleus in *Tetrahymena thermophila*. Genetics **154:**1587–1596.
30. **McCormick-Graham, M., and D. P. Romero.** 1996. A single telomerase RNA is sufficient for the synthesis of variable telomeric DNA repeats in ciliates of the genus *Paramecium*. Mol. Cell. Biol. **16:**1871–1879.
31. **McGrath, K. E., S. M. Yu, D. P. Heruth, A. A. Kelly, and M. A. Gorovsky.** 1994. Regulation and evolution of the single α-tubulin gene of the ciliate *Tetrahymena thermophila*. Cell Motil. Cytoskelet. **27:**272–283.
32. **Morris, N. R.** 2003. Nuclear positioning: the means is at the ends. Curr. Opin. Cell Biol. **15:**54–59.
33. **Munafo, D. B., and M. I. Colombo.** 2001. A novel assay to study autophagy: regulation of autophagosome vacuole size by amino acid deprivation. J. Cell Sci. **114:**3619–3629.
34. **Murata-Hori, M., and M. Fujishima.** 1996. Released substances from *Tetrahymena thermophila* arrest the cell cycle at G1 phase and removal of the substances induces highly synchronized cell division. Eur. J. Protistol. **32:**481–489.
35. **Nogales, E.** 2001. Structural insight into microtubule function. Annu. Rev. Biophys. Biomol. Struct. **30:**397–420.
36. **Orias, J. D., E. P. Hamilton, and E. Orias.** 1983. A microtubule meshwork associated with gametic pronucleus transfer across a cell-cell junction. Science **222:**181–184.
37. **Orr, G. A., P. Verdier-Pinard, H. McDaid, and S. B. Horwitz.** 2003. Mechanisms of taxol resistance related to microtubules. Oncogene **22:**7280–7295.
38. **Otto, G. P., M. Y. Wu, N. Kazgan, O. R. Anderson, and R. H. Kessin.** 2004. *Dictyostelium* macroautophagy mutants vary in the severity of their developmental defects. J. Biol. Chem. **279:**15621–15629.
39. **Petiot, A., E. Ogier-Denis, E. F. Blommaart, A. J. Meijer, and P. Codogno.** 2000. Distinct classes of phosphatidylinositol 3′-kinases are involved in signaling pathways that control macroautophagy in HT-29 cells. J. Biol. Chem. **275:**992–998.
40. **Rosenbaum, J.** 2000. Cytoskeleton: functions for tubulin modifications at last. Curr. Biol. **10:**R801–R803.
41. **Sawin, K. E., and T. J. Mitchison.** 1994. Microtubule flux in mitosis is independent of chromosomes, centrosomes, and antiparallel microtubules. Mol. Biol. Cell **5:**217–226.
42. **Schibler, M. J., and B. Huang.** 1991. The colR4 and colR15 β-tubulin mutations in *Chlamydomonas reinhardtii* confer altered sensitivities to microtubule inhibitors and herbicides by enhancing microtubule stability. J. Cell Biol. **113:**605–614.
43. **Surka, M. C., C. W. Tsang, and W. S. Trimble.** 2002. The mammalian septin MSF localizes with microtubules and is required for completion of cytokinesis. Mol. Biol. Cell **13:**3532–3545.
44. **Tamura, S., T. Tsuruhara, and Y. Watanabe.** 1969. Function of nuclear microtubules in macronuclear division of *Tetrahymena pyriformis*. Exp. Cell Res. **55:**351–358.
45. **Thazhath, R., C. Liu, and J. Gaertig.** 2002. Polyglycylation domain of β-tubulin maintains axonemal architecture and affects cytokinesis in *Tetrahymena*. Nat. Cell Biol. **4:**256–259.
46. **West, K. A., S. S. Castillo, and P. A. Dennis.** 2002. Activation of the PI3K/Akt pathway and chemotherapeutic resistance. Drug Resist. Updates **5:**234–248.
47. **Wilde, A., and Y. Zheng.** 1999. Stimulation of microtubule aster formation and spindle assembly by the small GTPase Ran. Science **284:**1359–1362.
48. **Williams, N. E.** 1984. Localizing surface-related proteins in cilates by indirect immunofluorescence microscopy. J. Protozool. **31:**492–494.
49. **Williams, N. E., and R. J. Williams.** 1976. Macronuclear division with and without microtubules in *Tetrahymena*. J. Cell Sci. **20:**61–77.
50. **Williams, S. A., R. E. Hosein, J. A. Garces, and R. H. Gavin.** 2000. *MYO1*, a novel, unconventional myosin gene affects endocytosis and macronuclear elongation in *Tetrahymena thermophila*. J. Eukaryot. Microbiol. **47:**561–568.
51. **Xia, L., B. Hai, Y. Gao, D. Burnette, R. Thazhath, J. Duan, M. H. Bre, N. Levilliers, M. A. Gorovsky, and J. Gaertig.** 2000. Polyglycylation of tubulin is essential and affects cell motility and division in *Tetrahymena thermophila*. J. Cell Biol. **149:**1097–1106.
52. **Yakisich, J., and G. Kapler.** The effect of phosphoinositide 3-kinase inhibitors on programmed nuclear degradation in *Tetrahymena* and fate of surviving nuclei. Cell Death Differ., in press.
53. **Yu, G. L., and E. H. Blackburn.** 1990. Amplification of tandemly repeated origin control sequences confers a replication advantage on rDNA replicons in *Tetrahymena thermophila*. Mol. Cell. Biol. **10:**2070–2080.